A novel *in vitro* model for studying the molecular mechanisms of amelogenesis in physiological and pathological conditions

PhD thesis

Thanyaporn Sang-ngoen

Doctoral School of Clinical Medicine

Semmelweis University

Supervisor: Gábor Varga, D.Sc.

Anna Földes, Ph.D.

Official reviewers: Balázs Sándor, D.M.D., Ph.D.

Hargita Hegyesi, Ph.D.

Head of the Complex Examination Committee: István Gera, D.M.D., Ph.D.

Members of the Complex Examination Committee: József Barabás, M.D., Ph.D.

Zoltán Rakonczay, D.Sc.

Budapest
2021

INTRODUCTION

Teeth are complex organs comprising of patterned mineralized and soft tissues. Teeth serve mastication and esthetic function. Once the tooth is damaged or lost, it could impact general well-being. Currently, tooth repair and replacement are based on artificial materials deficient in the natural tooth's biological characteristics. However, advanced science and technology lead us to a promising treatment to regenerate a tooth by using stem cells based on the knowledge of tooth development.

Enamel is produced during tooth development or odontogenesis, a multistep process requiring a complex reciprocal interaction between epithelial and ectomesenchymal cells. The process of dental enamel formation, technically called amelogenesis, is controlled by ameloblast cells which derive from the oral epithelium. Amelogenesis mainly comprises of two stages, secretory and maturation. During the secretory stage, ameloblasts primarily synthesize and secrete structural enamel matrix proteins initiating calcification and controlling the growth of enamel crystals. In the maturation stage, ameloblasts reduce the secretion of enamel matrix proteins and primarily play a role in the calcium and phosphate transportation resulting in high mineralization of enamel. In addition, ameloblasts regulate the pH where enamel development occurs. Since the formation of hydroxyapatite crystals generates a large number of protons, causing an acidic environment and could impede the crystal growth resulting in enamel developmental defects, e.g., hypomineralized enamel, abnormal enamel structure, etc.

The mechanism of amelogenesis and enamel developmental defect is still incompletely understood. The previous studies on amelogenesis are mainly based on histological and molecular techniques or animal models. Recently, a functional 2D model was developed for studying amelogenesis *in vitro*. This used HAT-7 ameloblast-like cells, originating from the rat incisor, that were cultured on Transwell permeable filters. HAT-7 cells exhibited maturation ameloblast characteristics, formed tight junctions, and were capable of the vectorial secretion of HCO_3^-. Although animal models can provide information related to the real physiological environment, the use of laboratory animals in functional studies is limited by technical difficulties and ethical concerns. To bridge the gap between 2D cell cultures and animal models, 3D cell culture systems have been developed recently. 3D cell culture systems are believed to provide results closer to those that would be obtained *in vivo*. Therefore, this project aimed to develop a 3D model of ameloblast cells, investigate the functional activity of HCO_3^- transporters, and test the toxicity of fluoride.

Objectives

1. To characterize the morphology of dental stem cells and HAT-7 ameloblast-like cells cultured by conventional 2D cell culture techniques.

2. To develop a 3D ameloblast model using HAT-7 cells grown in a Matrigel matrix and to evaluate three different culture media for their potential to allow spheroid formation.

3. To inspect the histological morphology of the spheroids by cryosection and staining with hematoxylin and eosin (H&E).

4. To investigate the gene expression of the maturation-stage ameloblast marker KLK4, the tight junction proteins cldn-1, cldn-4, cldn-8 and TJP1/ZO-1, and the electrolyte transporters involved in pH regulation for comparison with the previous 2D ameloblast model.

5. To functionally examine the activity of the electrolyte transporters regulating intracellular pH in 3D HAT-7 spheroids by microfluorometry.

6. To test the toxicity of a range of fluoride concentrations on the 3D ameloblast model.

Methods

Cell culture

Three dental tissues: residual parts of the dental follicle, periodontal ligament, dental pulp were isolated and collected from human impacted wisdom teeth as previously described (Perczel-Kovách et al., 2021). The isolated stem cells were resuspended in alpha modification of Eagle's medium (αMEM, Gibco) supplemented with 10% fetal bovine serum (FBS, Gibco), 2 mM L-glutamine (Sigma), 100 units/ml penicillin, and 100 mg/ml streptomycin (Gibco) and seeded in T75 tissue culture flasks (Orange Scientific). The cultures were maintained in an incubator under standard conditions (37 ˚C, 100 % humidity, 5 % CO_2), and the medium was changed twice a week.

HAT-7 cells were cultured with 'control medium', which is DMEM/F12 Ham medium (Sigma-Aldrich, St. Louis, MO, USA), 10% HyClone fetal bovine serum (Thermo Scientific, Waltham, MA, USA), 100 U/ml penicillin, and 10 μg/ml streptomycin (Sigma-Aldrich). When the cell confluence reached 70-80%, they were subcultured. The cultures were maintained in the same incubator as the stem cells, and the medium was replaced every other day.

HAT-7 cells were cultured on permeable polyester Transwell culture inserts with 0.4 μm pore size and 1.12 cm^2 surface area (Costar, Corning, NY, USA). The cells were fed with

a 'differentiation medium', which consists of a control medium (as explained above), $CaCl_2$ (2.1 mM final concentration), and 10^{-5} mM dexamethasone (Sigma-Aldrich).

Establishment of 3D cell model

HAT-7 cells were cultured in Matrigel® Basement Membrane Matrix (Corning, NY, United States) and fed with three different media: (1) control medium, (2) differentiation medium, 3) Hepato-STIM® (BD Biosciences, San Jose, CA, USA) supplemented with 10% HyClone fetal bovine serum (Thermo Scientific), 1% L-glutamine (Sigma-Aldrich), 100 U/ml penicillin and 10 g/ml streptomycin. Single suspended cells (~10,000 cells) in 20 µl of selected media were mixed with 50 µl of Matrigel matrix. After that, the mixing Matrigel matrix was placed in a 24-well Nunclon Sphera low-attachment plate (Thermo Fisher Scientific, Rochester, NY, USA). The plate was incubated at 37°C to let the Matrigel matrix solidify. Then 1 ml of the selected medium was added. The culture was maintained by incubating in a humidified atmosphere containing 5% CO_2 at 37°C, and the medium was replaced every other day. The change in cell growth and spheroid development was examined under a phase-contrast light microscopy (Nikon Eclipse TE200) and photos taken by a CCD camera (Blackfly USB3 CCD camera, FLIR Systems, Wilsonville, OR, USA).

Histological section

HAT-7 spheroids grown for 7 days in Matrigel with Hepato-STIM medium were isolated by trypsinization with 0.25% Trypsin/EDTA. Then the spheroids were fixed by 4% PFA (in PBS). After an hour, the spheroids were kept in 10% w/v sucrose solution until the embedding process. The spheroids were embedded in cryomatrix (Thermo Shandon Limited, Cheshire WA7 1TA, UK) before cutting at 5 µm with cryostat machine (Leica CM3050 S, Leica Biosystems Division of Leica Microsystems Inc., IL, USA).

Quantitative real-time PCR analysis

The gene expressions of HAT-7 spheroids at day 7 were assessed compared to HAT-7 cells cultured on Transwell permeable supports. The process began with total RNA extraction using a GeneJET RNA Purification Kit (Thermo Scientific), and the concentration was measured with a NanoDrop ND-1000 spectrophotometer (NanoDrop Technologies). After that, 1.5 µg of total RNA per sample was reverse transcribed to cDNA (in 20 µl) by means of a Maxima First Strand cDNA Synthesis Kit for RT-qPCR (Thermo Scientific). TaqMan Universal Master Mix II (Applied Biosystems, Foster City, CA, USA) and predesigned primers (Life Technologies Magyarország Kft., Budapest) were applied in a final volume of 20 µl for amplification. Relative fold changes in gene expression were calculated using the comparative

Ct method (2−ΔΔCT) and each relative fold change value of each experimental condition was measured from three parallels.

Microfluorometry

HAT-7 spheroids grown in Hepato-STIM medium for one week were isolated from the Matrigel and plated on coverslips coated with 0.01% poly-L-lysine solution (Sigma-Aldrich). BCECF-AM fluorescent dye (3 μM, Molecular Probes, Eugene, OR, United States) was loaded into the spheroids for an hour at 37°C. After that, coverslips were mounted in a purpose-built perfusion chamber. A HEPES-buffered solution or bicarbonate buffered bath solution was perfused through the spheroids at 0.9 ml/min. The activities of specific electrolyte transporters were investigated by applying ions withdrawal substances and transporter specific inhibitors. The signals were obtained at 530 nm with two excitation wavelengths (490 and 440 nm) and converted to pH_i using calibration data obtained with the nigericin/high potassium method.

Fluoride exposure

The experiments were divided into two groups. For the first group, the Hepato-STIM medium was replaced by Hepato-STIM medium containing 0 (control), 0.1, 0.3, 1.0, or 3.0 mM fluoride after a day of cell seeding in Matrigel. For the second group, the medium was replaced by Hepato-STIM, containing the same range of fluoride concentrations, on day 4 of cell seeding. In both groups, the medium was changed every other day.

Statistical Analysis

Where appropriate, data are presented as mean ± SEM. Statistical analyses were performed using either one-sample t-tests or analysis of variance combined with Tukey's multiple comparison test as appropriate.

Results

Morphology of human dental mesenchymal stem cells and rat HAT-7 cell line

At the time of the stem cell seeding, the cells were spherical. After attachment the cells became elongated and flattened, and showed a spindle or fibroblast-like shape. They retained this morphology and proliferated until confluence was reached. The number of viable cells, of all three stem cell types, cultured in both control and differentiation media, increased continuously. Hence the dental stem cells maintained the cell viability although the cell density was high.

At the time of HAT-7 cell seeding, the cells had a spherical shape. After a few days, the cells showed a fairly uniform polygonal shape with distinct cell borders giving a

cobblestone appearance typical of epithelial cells. When HAT-7 cells were grown on permeable Transwell supports, their appearance was similar to HAT-7 cells grown in plastic flasks.

3D culture of HAT-7 cells with basement membrane matrix

The spheroid development in three different culture media was observed across two weeks. Initially, the cells in different three culture media were relatively uniform in size. After three days of cell seeding, the size and appearance of the cells slightly change. After a week, some of the cells cultured in the control and differentiation medium show signs of division. And after two weeks, most of the cells remained the similar size and appearance as at the beginning. Only a few became larger and developed to a multicellular spherical structure.

In contrast, the cells grown in Hepato-STIM medium proliferated and developed into multicellular spherical appearance much more quickly and persistently after three days of culture. Within one week, many spheroids, which were approximately 100 μm in diameter, had developed. When the culture was continued, the spheroids had become huge and begun to disintegrate. Therefore, the spheroids developed in Hepato-STIM for one week was used for other experiment method examining molecular components and functional activity.

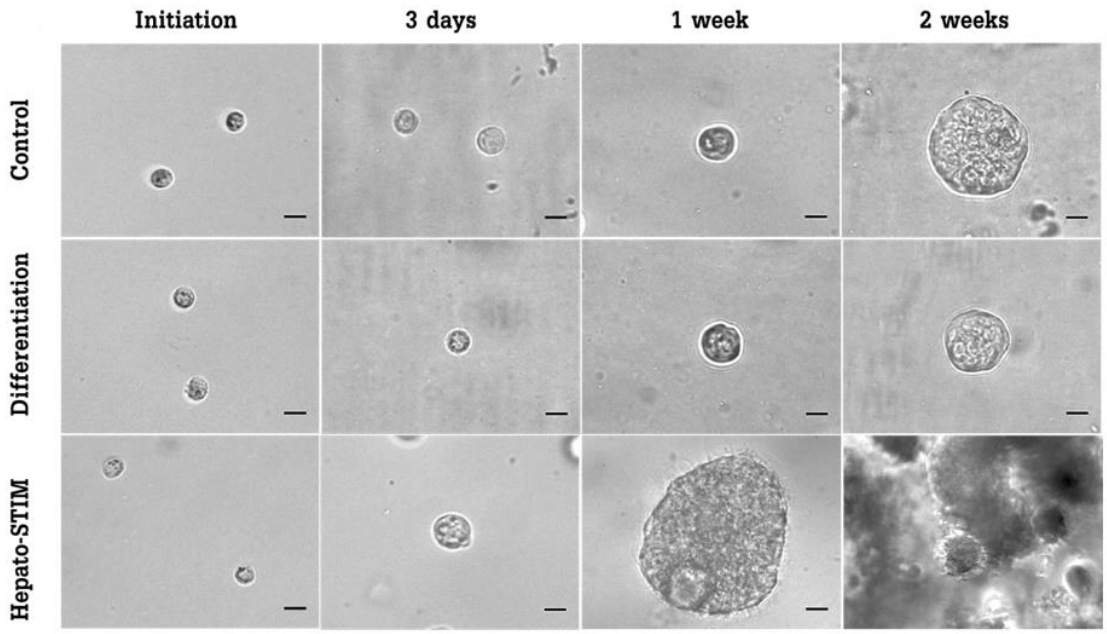

Figure 1. *HAT-7 spheroid development in Matrigel matrix. Morphology of HAT-7 cells cultured with three different culture media: control, differentiation, and Hepato-STIM. The growth and spheroid development of HAT-7 cells in each medium was displayed on the day of seeding, and after 3 days, 1 week and 2 weeks. Scale bars: 20 μm.*

Histological morphology

The morphology of the spheroids varied considerably. The small spheroids were around 70 μm in diameter and contained a dense aggregation of undifferentiated cells with randomly distributed small pools of extracellular fluid or 'lacunae'. The intermediate sized spheroids were around 100 μm in diameter. They contained significant numbers of lacunae and presented an emerging outer epithelial layer connected in several places to the central cell mass. The largest spheroids exhibited an outer epithelial monolayer wholly separated from a central cell mass by a clear fluid-filled space or lumen. The central cell mass was either disorganized and undifferentiated or had a lamellar structure.

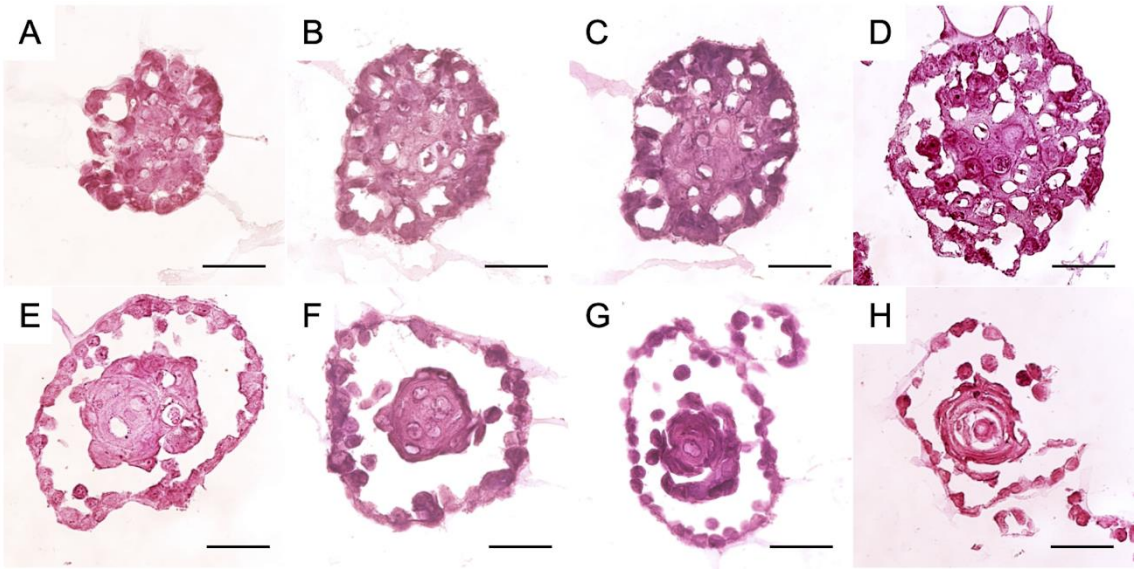

Figure 2. *Morphology of HAT-7 spheroids cultured in Matrigel matrix with Hepato-STIM medium for seven days. Spheroids were released from the matrix and processed for cryosection. The sections were cut at 5-μm thickness and stained with hematoxylin and eosin. Scale bars: 50 μm.*

Gene expression of ameloblast markers, tight junction proteins and transporters

RNA was extracted from HAT-7 spheroids grown in Matrigel matrix with Hepato-STIM medium for a week (our preferred model) and from HAT-7 monolayers grown on Transwell permeable supports. Data from both sample groups were compared to detect any significant differences in gene expression level between the previous 2D cultures and this 3D HAT-7 cell model. The highest expression level among the chosen genes was KLK4, a maturation-stage ameloblast marker. The expression level of KLK4 in the spheroids was approximately 70-fold greater than in the 2D HAT-7 model. Of the four tight-junction proteins

examined, only cldn-8 was significantly increased in HAT-7 spheroids compared to the 2D model. Expression levels of the other three, cldn-1, cldn-4 and TJP1/ZO-1, were significantly decreased in the spheroids compared to the 2D model. Most of the electrolyte transporters involved in HCO_3^- secretion by maturation-stage ameloblasts, SLC9A1/NHE1, SLC4A2/AE2 and SLC4A4/NBCe1, were detected in the HAT-7 spheroids but were expressed at slightly lower levels than in the 2D model. Interestingly, the other two transporters, SLC26A4/pendrin, and CFTR, generally located on the apical membrane, were significantly reduce in the spheroids compared to the 2D model.

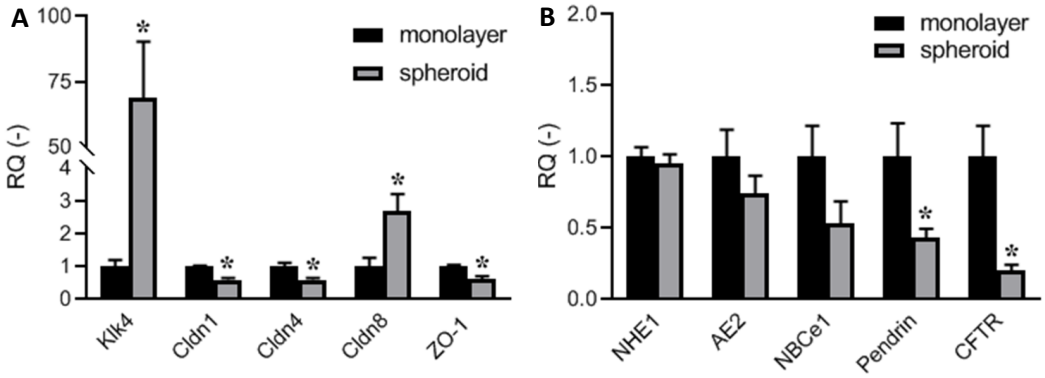

Figure 3. *Quantitative RT-PCR data indicating gene expression levels in HAT-7 spheroids cultured in Matrigel matrix with Hepato-STIM medium for seven days, normalized to the corresponding 2D monolayer culture data. (A) expression of the maturation-stage ameloblast marker gene KLK4 and the tight-junction protein genes, cldn-1, cldn-4, cldn-8 and Tjp1 (ZO-1). (B) expression of electrolyte transporter genes Slc9a1 (NHE1), Slc4a2 (AE2), Slc4a4 (NBCe1), Slc26a4 (pendrin) and Cftr (CFTR). Data presented as mean ± SEM. *p < 0.05 (n = 4).*

Intracellular pH regulation

To assess Na^+-H^+ exchanger activity in the spheroid cells, the rate of pH_i recovery from the acid loading induced by exposure to an ammonium pulse was measured in a HCO_3^--free, HEPES-buffered physiological salt solution. HAT-7 spheroids were exposed to 20 mM NH_4Cl for 3 minutes resulting in a transient alkalinization of the cells before a quick, rapid drop in pH_i to a markedly acidic value. This intracellular acidification was sustained in the absence of Na^+ by substitution of extracellular Na^+ with $NMDG^+$. This showed that the cells were unable to extrude H^+ from the cells without Na^+. In other words, the spheroid cells have no Na^+-independent pathway for extruding H^+, such as an H^+-ATPase. When Na^+ was restored, pH_i

quickly recovered to control values. This indicates Na^+ is required to extrude H^+, so there might be a Na^+-dependent H^+ extruder in HAT-7 spheroids. This was confirmed by repeating the procedure and restoring Na^+ in the presence of a selective inhibitor of Na^+/H^+ exchanger, amiloride (0.3 mM). The rate of pH_i recovery from acidification was greatly decreased. Thus, an Na^+/H^+ exchanger, most likely to be NHE1, exists in HAT-7 spheroids.

To assess the activity of Na^+-HCO_3^- cotransporters in the spheroids, the above process was repeated, but this time in a bath solution containing HCO_3^-. When Na^+ was restored after the intracellular acidification in the presence of amiloride, the recovery from acidification was not completely inhibited by amiloride. This HCO_3^-- and Na^+-dependent component of the recovery from acidification is most likely due to a HCO_3^-- and Na^+-dependent transporter such as an Na^+-HCO_3^- cotransporter. When Na^+ was restored in the presence of both amiloride and H_2DIDS (0.5 mM) - an inhibitor of Na^+- HCO_3^- cotransport - the inhibition of pH_i recovery was more potent than that due to amiloride alone. This suggests that a Na^+- HCO_3^- cotransporter, most likely to be NBCe1, is active in HAT-7 spheroids.

To assess the activity of anion exchangers in HAT-7 spheroid cells, extracellular Cl^- in the HCO_3^--buffered bath solution was substituted with gluconate and the resulting changes in pH_i were measured. Extracellular Cl^- withdrawal reverses the existing concentration gradient of Cl^-, which would result in Cl^- efflux from the cells driving an influx of HCO_3^-, and a rise in pH_i, if anion exchangers were active in the HAT-7 spheroid cells. As expected, a notable increase in pH_i in the spheroid cells could be detected. When Cl^- was restored to the bath solution, pH_i returned to the normal value. When the experiment was repeated in the presence of 0.1 mM DIDS, an inhibitor of Cl^-/HCO_3^- exchange, the rate of change in pH_i was clearly reduced. This suggests the presence of an active Cl^-/ HCO_3^- exchanger, most probably AE2, in HAT-7 spheroids.

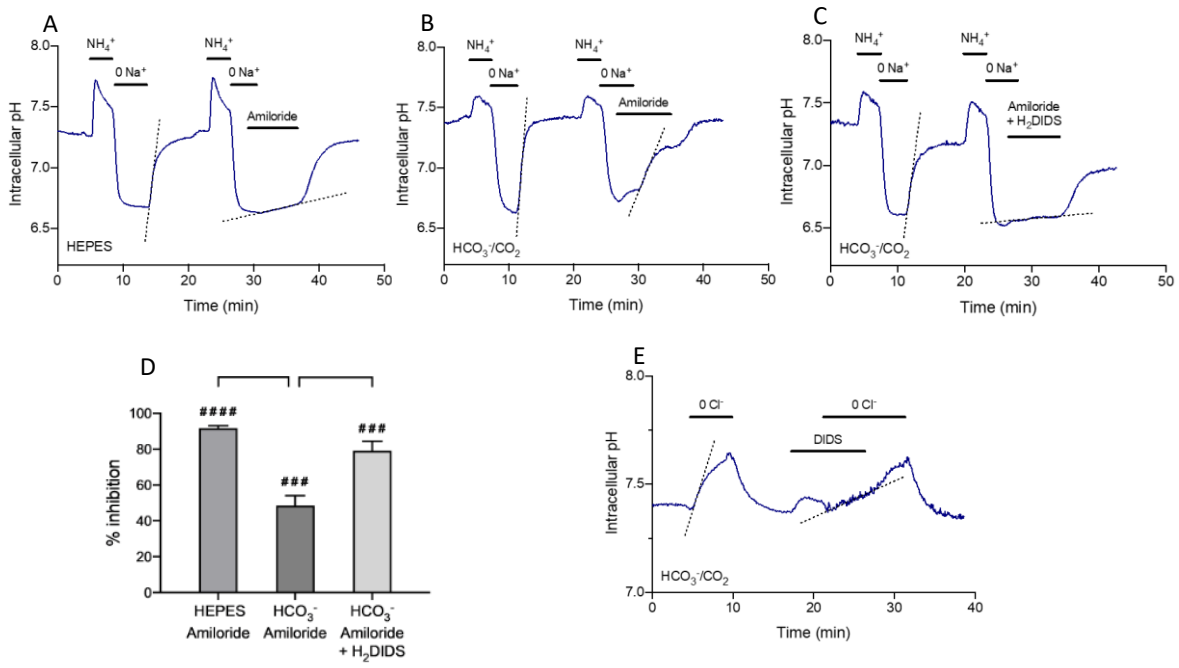

Figure 4. *Changes in pH_i of HAT-7 spheroids measured by microfluorimetry. (A-C) Recovery of pH_i from intracellular acidification. The spheroids were exposed to 20 mM NH_4^+ for 3 minutes, followed by extracellular Na^+ withdrawal by replacement with $NMDG^+$ (0 Na^+): (A) in HEPES-buffered bath solution with and without 0.3 mM amiloride; (B) in HCO_3^--buffered bath solution with and without 0.3 mM amiloride; (C) in HCO3-buffered bath solution with or without a combination of 0.3 mM amiloride and 0.5 mM H_2DIDS. (D) The average percentage inhibition of pH_i recovery rate in the presence of amiloride with or without H_2DIDS and with or without HCO_3^-. Mean (± SEM) calculated from 4-6 experiments with reference to the internal control in each experiment. ####p < 0.0001, ###p < 0.001 compared with control (one-sample t-test). (E) The increase in pH_i induced by substituting extracellular Cl^- with gluconate (0Cl^-) in a HCO_3^--buffered bath solution with or without 0.1 mM DIDS. The rates of change of pH_i when Na^+ was restored (A-C) or Cl^- removed (E) are shown as dashed lines.*

Fluoride exposure

An experiment to investigate the effect of fluoride on HAT-7 spheroids comprised a control group that was not exposed to fluoride and an experimental group exposed to a range of fluoride concentrations: 0.1, 0.3, 1.0 and 3.0 mM. In the first series, fluoride was added to the medium after 24 hours when the cells were already embedded in the Matrigel matrix. The HAT-7 cells grew and formed spheroids quickly and uniformly in the control group. HAT-7 cells exposed to 0.1 and 0.3 mM fluoride were also able to form spheroids that were similar in

size and appearance to the control group. On day 7, spheroids released from the matrix also retained the same size and appearance as the control group. Therefore, 0.1 and 0.3 mM fluoride did not visibly affect cell proliferation and spheroid formation. In the 1 mM fluoride medium, however, only a few HAT-7 cells were able to develop into spheroids, and the size of these spheroids was smaller than those in the control group or lower fluoride concentration groups. A large number of cells died and were seen as cellular debris. On day 7, those few spheroids that were released from the matrix remained smaller than the control group. Only a few HAT-7 cells exposed to 3 mM fluoride survived, and no spheroids developed.

In the second series, fluoride was introduced on day 4 when the HAT-7 cells had already established a multicellular spherical appearance and had started enlarging rapidly. HAT-7 spheroids exposed to 0.1 and 0.3 mM fluoride retained their ability to proliferate and the spheroids grew in size. The size and number of the spheroids, including their growth rate, were similar to those grown in the control medium. Thus again, 0.1 and 0.3 mM fluoride had little or no effect on the growth of the spheroids. As in the first series of experiments, the higher fluoride concentrations (1 mM and 3 mM), when introduced on day 4, more visibly affect spheroid growth. In the presence of 1 mM fluoride, the existing spheroids gradually decreased in size and were disaggregating by day 7. This effect was also noticeable when the spheroids were isolated from the matrix. Only a few intact spheroids were seen while a lot of cell debris was present. This was also observed in the spheroids exposed to 3 mM fluoride, but the death and disintegration of the spheroids developed more quickly, and no spheroids were seen by day 7.

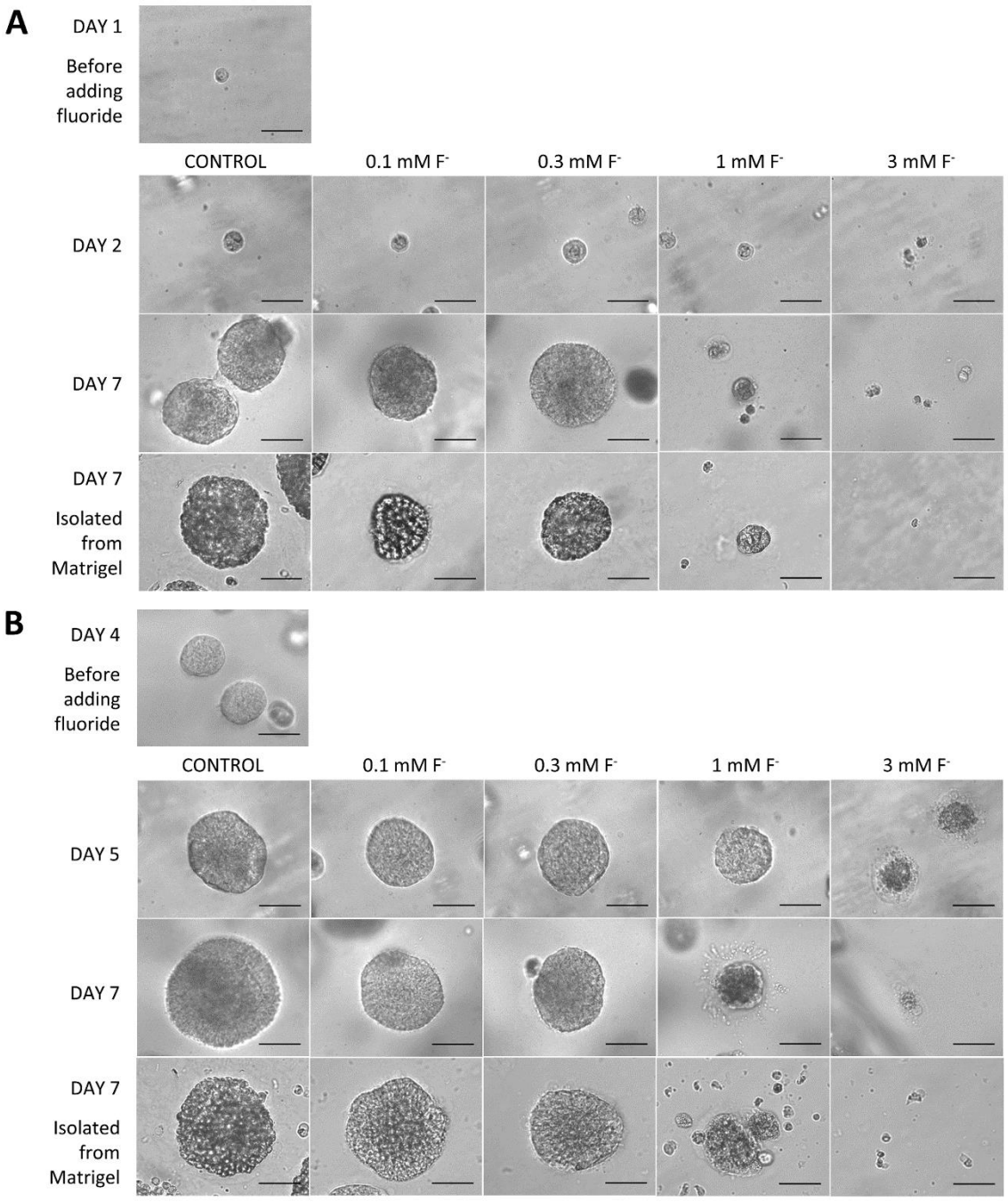

Figure 5. *Morphology of HAT-7 spheroids cultured in Matrigel matrix with Hepato-STIM medium containing 0 mM (control), 0.1, 0.3, 1 and 3 mM fluoride. (A) Spheroid appearance on days 1, 2 and 7 when the fluoride was introduced 24 hours after cell embedding in the matrix. (B) Spheroid appearance on days 4, 5 and 7 when fluoride was introduced on day 4 after the spheroids had already formed. The appearance of spheroids isolated from the matrix on day 7 is also shown. Scale bars: 70 μm.*

Conclusions

1) Dental stem cells and HAT-7 ameloblast-like cells established different cell morphologies *in vitro*. Dental stem cells showed a fibroblast-like appearance indicating mesenchymal characteristics. HAT-7 cells showed a polygonal, cobble-stone appearance, which is characteristic of epithelial cells.

2) This 3D ameloblast model has been successfully achieved by culturing HAT-7 cells in Matrigel matrix and by feeding with Hepato-STIM medium.

3) HAT-7 spheroids showed the potential for morphogenesis by forming multicellular structures and contained a lumen.

4) HAT-7 spheroids expressed the maturation-ameloblast marker KLK4, tight junction proteins and basic electrolyte transporters.

5) HAT-7 spheroids demonstrated the capacity for intracellular pH regulation by the verified activity of key $H+/HCO_3^-$ transporters.

6) In the 3D HAT-7 model, the result depends on the concentration of fluoride.

In summary, this new experimental model provides a basis for better understanding amelogenesis and it hints at the potential of 3D ameloblast organoids for tissue repair and/or tooth regeneration.

Bibliography

Publications related to the thesis

1. Földes, A., **Sang-Ngoen, T.**, Kádár, K., Rácz, R., Zsembery, Á., DenBesten, P., Steward, M. C., & Varga, G. (2021). Three-Dimensional Culture of Ameloblast-Originated HAT-7 Cells for Functional Modeling of Defective Tooth Enamel Formation. Frontiers in pharmacology, 12, 682654. https://doi.org/10.3389/fphar.2021.682654

2. Perczel-Kovách, K., Hegedűs, O., Földes, A., **Sangngoen, T.**, Kálló, K., Steward, M. C., Varga, G., & Nagy, K. S. (2021). STRO-1 positive cell expansion during osteogenic differentiation: A comparative study of three mesenchymal stem cell types of dental origin. Archives of oral biology, 122, 104995. https://doi.org/10.1016/j.archoralbio.2020.104995

Publications unrelated to the thesis

1. Ruksakiet, K., Hanák, L., Farkas, N., Hegyi, P., Sadaeng, W., Czumbel, L. M., **Sang-Ngoen, T.**, Garami, A., Mikó, A., Varga, G., & Lohinai, Z. (2020). Antimicrobial Efficacy of Chlorhexidine and Sodium Hypochlorite in Root Canal Disinfection: A Systematic Review and Meta-analysis of Randomized Controlled Trials. Journal of endodontics, 46(8), 1032–1041.e7. https://doi.org/10.1016/j.joen.2020.05.002

2. Sadaeng, W., Márta, K., Mátrai, P., Hegyi, P., Tóth, B., Németh, B., Czumbel, L. M., **Sang-Ngoen, T.**, Gyöngyi, Z., Varga, G., Révész, P., Szanyi, I., Karádi, K., & Gerber, G. (2020). γ-Aminobutyric Acid and Derivatives Reduce the Incidence of Acute Pain after Herpes Zoster - A Systematic Review and Meta-analysis. Current pharmaceutical design, 26(25), 3026–3038. https://doi.org/10.2174/1381612826666200605120242

3. Csupor, D., Viczián, R., Lantos, T., Kiss, T., Hegyi, P., Tenk, J., Czumbel, L. M., **Thanyaporn, S. N.**, Gyöngyi, Z., Varga, G., Gerber, G., Pétervári, E., & Tóth, B. (2019). The combination of hawthorn extract and camphor significantly increases blood pressure: A meta-analysis and systematic review. Phytomedicine : international journal of phytotherapy and phytopharmacology, 63, 152984. https://doi.org/10.1016/j.phymed.2019.152984